Journal of Theoretical Biology 588 (2024) 111835

Contents lists available at ScienceDirect

Journal of Theoretical Biology

journal homepage: www.elsevier.com/locate/yjtbi

Adipose tissue in the small airways: How much is enough to drive functional changes?

Graham M. Donovan [a,*], Carolyn J. Wang [b], Peter B. Noble [b], Kimberley C.W. Wang [b,c]

[a] Department of Mathematics, University of Auckland, Auckland, 1142, New Zealand
[b] School of Human Sciences, The University of Western Australia, Crawley, 6009, Western Australia, Australia
[c] Telethon Kids Institute, The University of Western Australia, Nedlands, 6009, Western Australia, Australia

ARTICLE INFO

Keywords:
Bronchoconstriction
Obesity
Asthma
Airway remodelling
Airway hyper-responsiveness
Adipose tissue

ABSTRACT

Obesity is a contributing factor to asthma severity; while it has long been understood that obesity is related to greater asthma burden, the mechanisms though which this occurs have not been fully elucidated. One common explanation is that obesity mechanically reduces lung volume through accumulation of adipose tissue external to the thoracic cavity. However, it has been recently demonstrated that there is substantial adipose tissue within the airway wall itself, and that the presence of adipose tissue within the airway wall is related to body mass index. This suggests the possibility of an additional mechanism by which obesity may worsen asthma, namely by altering the behaviour of the airways themselves. To this end, we modify Anafi & Wilson's classic model of the bistable terminal airway to incorporate adipose tissue within the airway wall in order to answer the question of how much adipose tissue would be required in order to drive substantive functional changes. This analysis suggests that adipose tissue within the airway wall on the order of 1%–2% of total airway cross-sectional area could be sufficient to drive meaningful changes, and further that these changes may interact with volume effects to magnify the overall burden.

1. Introduction

Asthma is characterised by multiple processes which together serve to limit flow through the conducting airways; these include inflammation and airway wall remodelling, as well as reversible airway narrowing driven by constriction of the band of airway smooth muscle surrounding the airways (Wang et al., 2020). Obesity is a significant co-morbidity which often occurs alongside, and is related to greater asthma burden (Beuther and Sutherland, 2007; Farah and Salome, 2012). However, the mechanism through which this occurs is unclear. Perhaps the most commonly cited explanation is that obesity reduces lung volume and thus external load on the airways (Skloot et al., 2011; Bates, 2016).

A more recent finding is the presence of substantial adipose tissue within the airway wall itself in large airways in humans, and that the amount of adipose tissue is related to body mass index (BMI) (Elliot et al., 2019). Airway-associated adipose tissue is also present throughout the airway tree (both large and small airways) in animal models, and it is biologically active (Wang et al., 2023a,b). These findings suggest the possibility of an additional mechanism by which obesity may worsen asthma, namely that the presence of adipose tissue within the airway wall alters the behaviour of the airway itself.

The dynamics of airway narrowing are important in understanding lung function in asthma. In particular, the smallest conducting (terminal) airways are thought to exhibit a bistability in which, for a fixed input pressure, an airway may be either effectively open, or effectively closed (Anafi and Wilson, 2001; Donovan, 2023). This instability is thought to arise from interdependence between the airway and the parenchyma in which it is embedded, because of the tethering attachments between parenchyma and airway, and the dependence of the inflation of the parenchyma on the flow through the airway. The patterns in which this airway closure is organised lead to so-called *ventilation defects* (Anafi and Wilson, 2001; Venegas et al., 2005; Donovan, 2016, 2017) which are a cardinal feature of asthma. Although one should take care with over-emphasising the distinction between small and large airways (Donovan and Noble, 2021), it is also true that the small airways play a key role in asthma (Tgavalekos et al., 2005). The bistability mechanism described above was originally formulated in terms of the smallest conducting airways (the terminal airways) in Anafi and Wilson (2001), and this is also the focus of the present paper, though a similar concept has also been applied in more proximal airways as well Venegas et al. (2005).

* Corresponding author.
E-mail address: g.donovan@auckland.ac.nz (G.M. Donovan).

https://doi.org/10.1016/j.jtbi.2024.111835
Received 17 October 2023; Received in revised form 27 March 2024; Accepted 17 April 2024
Available online 20 April 2024

One key question, then is how the addition of adipose tissue to the airway wall itself might alter the function of the airways. This could manifest in two distinct ways: (i) by thickening the airway wall and displacing tissue inward, directly impinging upon the airway lumen and restricting airflow, or (ii) by thickening outward and reducing the restoring forces of the parenchymal tethering, leading indirectly to greater narrowing under constriction. In this manuscript we will modify the model of Anafi and Wilson (2001) to accommodate both types of alteration due to adipose tissue in order to understand how different levels of adipose tissue within the airway wall might affect airway and lung function in asthma.

The focus of this study is the smaller, distal airways, in which the bistability mechanism was originally proposed. While adipose tissue has been found in the airway wall in larger human airways (Elliot et al., 2019), it has so far not been detected in small airways in humans. More recent animal studies, however, have shown adipose tissue throughout the airway tree (Wang et al., 2023a,b). Thus, at the present time, the precise amount of adipose tissue in the human small airways, and/or other obesity-associated airway remodelling in these airways, is unknown. Our goal here is to establish, through use of a mathematical model, the boundaries at which such adipose tissue, or other remodelling, would begin to have significant functional consequences — for example in terms of airway tree resistance or airway closure.

2. Model

In this section we review the model of Anafi and Wilson (2001) and describe the modifications for incorporation of adipose tissue in the airway wall. The basic geometry is given in Fig. 1, showing the maximum airway size r_0 and the three radii normalised to this: ρ_i as the inner (luminal) radius, ρ_m as the radius of the airway smooth muscle, and ρ_{adi} as the outer boundary at which the parenchymal tethering attachments generate the restoring force. The cross-sectional fraction of the submucosa is given by f (relative to the unconstricted airway area) and so

$$\rho_i^2 = \rho_m^2 - f \tag{1}$$

and similarly the additional cross-sectional fraction due to adipose tissue, in an outward direction (f_{adi}), leads to

$$\rho_{adi}^2 = \rho_m^2 + f_{adi}. \tag{2}$$

Note that if one sets $f_{adi} = 0$ then the original (Anafi and Wilson, 2001) model is recovered.

Flow through the airway is described by a Poiseuille-type flow where the resistance is given by

$$R_{aw} = \frac{12 l \mu}{\pi r_o^4 \rho_i^4} \tag{3}$$

where l is the airway length, μ is the gas viscosity, and $r_o\rho_i$ is (as before) the luminal radius.

The airway entrance pressure is assumed to be sinusoidal about a mean pressure $\bar{P}$ with amplitude $\|P_{aw}\|$ and frequency ω as

$$P_{aw}(t) = \bar{P} + \|P_{aw}\| \sin(\omega t). \tag{4}$$

Under the assumption that the airway resistance (R_{aw}) and parenchymal elastance (E) are nearly constant during a breathing cycle, the alveolar pressure will also be sinusoidal as

$$P_A(t) = \bar{P} + \|P_A\| \sin(\omega t - \alpha) \tag{5}$$

with amplitude

$$\|P_A\| = \|P_{aw}\| \frac{E}{\sqrt{E^2 + (\omega R_{aw})^2}} \tag{6}$$

and phase lag

$$\alpha = \tan^{-1}\left(\frac{\omega R_{aw}}{E}\right). \tag{7}$$

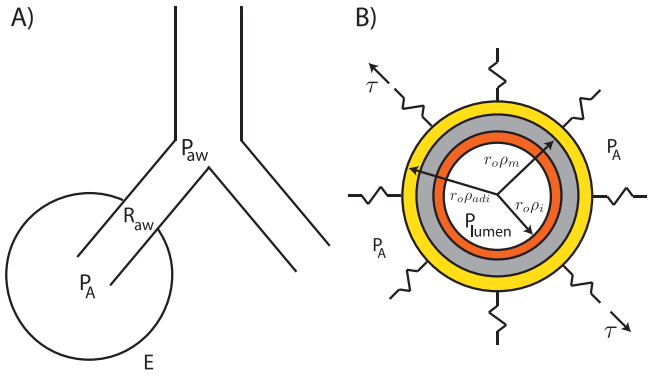

Fig. 1. Model schematic. Panel A: terminal airway and alveolus, showing airway entrance pressure (P_{aw}), alveolar pressure (P_A), airway resistance (R_{aw}) and parenchymal elastance (E). Panel B: cross-section of the airway, illustrating the dimensional maximum airway size at total lung capacity (TLC) (r_0) and the nondimensional radii referenced to this for the luminal radius ρ_i, smooth muscle radius ρ_m, and external (adipose tissue) radius ρ_{adi}. The pressure inside the lumen is P_{lumen} and τ gives the parenchymal tethering stress. Relative to the reference model, inward adipose tissue is represented as the orange band, and outward in yellow.

The pressure balance across the airway wall requires that

$$\frac{T}{r_0\rho_m} = P_{tm} \tag{8}$$

where T is the tension due to the airway smooth muscle[1] and P_{tm} is the transmural pressure. (The $(1/r)$-type dependence on the left-hand side arises from Laplace's law.) The transmural pressure must also balance the difference between the luminal pressure P_{lumen} and the alveolar pressure P_A, and furthermore the parenchymal tethering stress[2] τ so that

$$P_{tm} = P_{lumen} - P_A + \tau. \tag{9}$$

The luminal pressure is taken at the airway midpoint and so

$$P_{lumen} = (P_{aw} + P_A)/2. \tag{10}$$

The treatment of the parenchymal tethering stress follows Lai-Fook (1979), in which τ depends both on distortion of the parenchyma (due to airway narrowing) and P_A. The (dimensionless) deviation from the undeformed "hole" in the parenchyma (at total lung capacity (TLC)) in which the airway sits is thus described as

$$x = 1 - \frac{\rho_{adi}}{\sqrt[3]{v}} \tag{11}$$

assuming isotropic expansion and contraction in proportion to the cube root of volume. The acinar volume is the sum of the residual volume V_{RV} and the elastic expansion P_A/E so that we have

$$v = \frac{V_{RV} + (P_A/E)}{V_{TLC}} \tag{12}$$

when normalised to total lung capacity (V_{TLC}). As per Lai-Fook (1979), parenchymal tethering is then described as

$$\tau = P_A(1 + 1.4x + 2.1x^2). \tag{13}$$

Observe that we have modified the original model formulation such that the parenchymal attachments are at $r_0\rho_{adi}$, rather than at $r_0\rho_m$ as in the original. Because $\rho_{adi} \geq \rho_m$ this serves to decrease the effect of the parenchymal attachments (e.g. Macklem, 1996) which will

[1] In the tangential direction, assuming circumferential arrangement of the smooth muscle.

[2] Here we follow the notational conventions of Anafi and Wilson (2001) and Lai-Fook (1979), but note that the units of τ are the same as the units of P_A (see Eq. (13)).

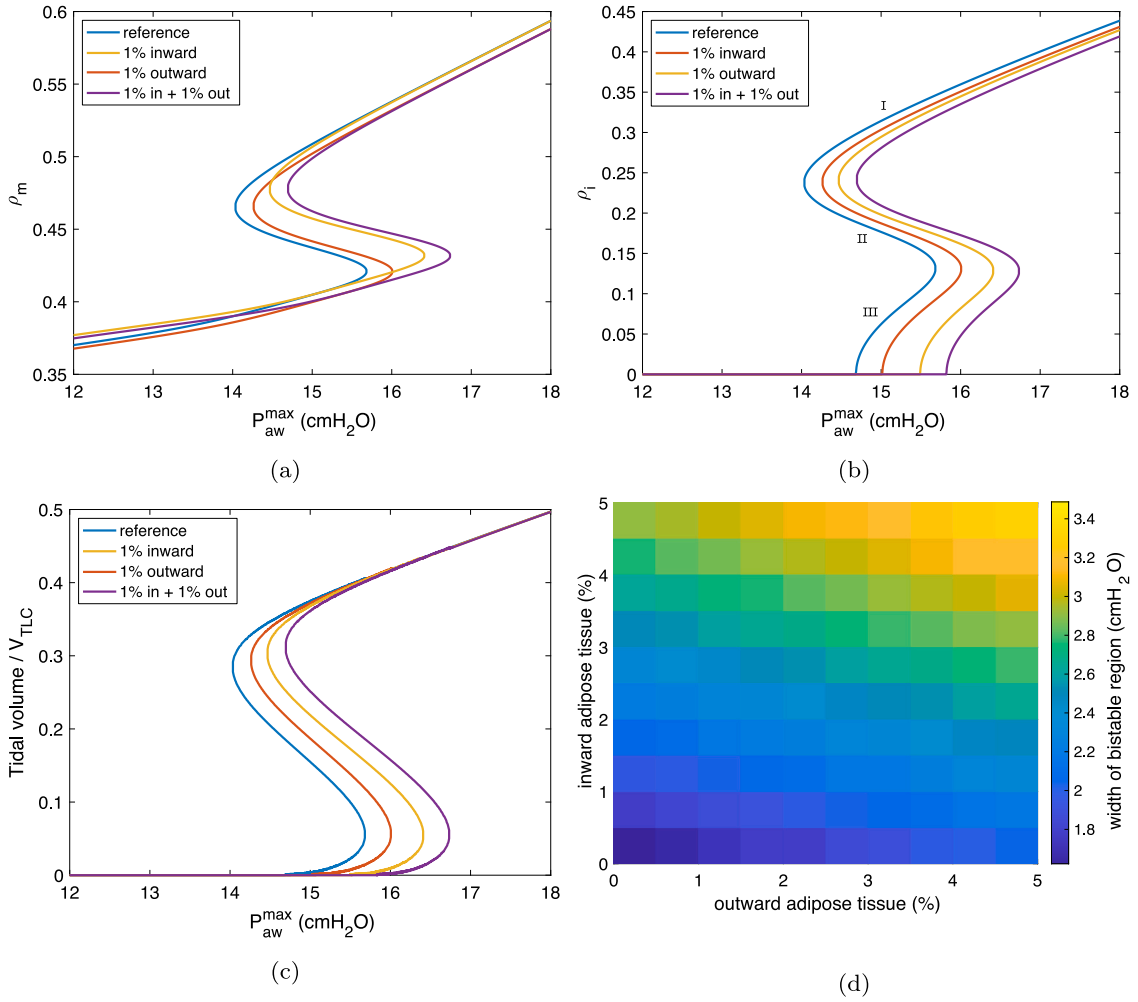

Fig. 2. Model solutions. Panels (a)–(c) illustrate how airway quantities (panel a, ρ_m; (b), ρ_i and (c), tidal volume) change as P_{aw}^{max} varies, and how this is altered by various degrees of adipose tissue (see legends). The region of bistability is apparent, with an effectively open state in which the tidal volume is $\approx 40\%$ of V_{TLC} (region I in panel (b)), a closed state in which the volume is effectively zero (III), and an intermediate state (II, in which the flow equations are unstable). The regions are the same in panels (a)–(c) but only explicitly labelled in (b). Panel (d) shows in more detail how the width of this region of bistability varies (i.e. over which region II exists) for different levels of combined inward and outward adipose tissue.

ultimately allow for greater narrowing under bronchoconstriction due to a reduction in opposing forces. If $f_{adi} = 0$ then $\rho_{adi} = \rho_m$ and the original model is fully recovered.

Finally a very simple description of the maximum airway smooth muscle tension T_{max} completes the model, with the affine approximation

$$\frac{T_{max}}{T_o} = 1.25\rho_m - 0.25 \tag{14}$$

where T_o is the isometric tension at optimal length. The origin of this approximate constitutive law is described in Anafi and Wilson (2001); it is a very simple description of ASM, which exhibits many complex behaviours (cf. Mijailovich et al., 2000; Bates et al., 2009), but serves to approximate the maximum value reasonably well.

Thus, under the assumption that both maxima (that is, T_{max} and P_{tm}^{max}) occur at the same part of the breathing cycle, we have

$$\frac{T_o(1.25\rho_m - 0.25)}{r_o\rho_m} = P_{tm}^{max} \tag{15}$$

where

$$P_{tm}^{max} = \max_t P_{tm}(t). \tag{16}$$

All parameter values are taken from Anafi and Wilson (2001). In particular, this implies that the lung is under positive end-expiratory pressure (PEEP), i.e. that $\|P_{aw}\| = (P_{aw}^{max} - \text{PEEP})/2$. The other parameter values are $T_0/r_0 = 40$ cm H_2O, $\omega = 0.33$ Hz, $E = 25$ kPa/ml, $l = 0.3$ cm, $f = 16\%$, $r_0 = 0.027$ cm, and $V_{RV} = 20\%\, V_{TLC}$. Outward displacement of the airway wall due to adipose tissue is then incorporated by the parameter f_{adi}; inward displacement is simply reflected by an increase f from the reference value.

3. Results

Model solutions[3] as P_{aw}^{max} is varied are shown in Fig. 2. Panels (a)–(c) show properties of the airway as P_{aw}^{max} is varied, in particular the muscle radius ρ_m in (a), the luminal radius ρ_i in (b), and the resulting tidal volume over a breathing cycle in (c). In all three panels the region of bistability is apparent, in which for a fixed value of P_{aw}^{max} there exists an effectively open state in which the tidal volume is $\approx 40\%$ of V_{TLC}, a closed state in which the tidal volume is effectively zero, and an intermediate state (in which the flow equations are unstable). These regions are labelled illustratively in panel (b) as I, II and III respectively.

Changes in the width of this region of bistability are shown in panel (d), as the inward and outward adipose tissue fractions are varied. In the bottom left corner the reference model (0% adipose

[3] We will discuss in the next section how these solutions are found.

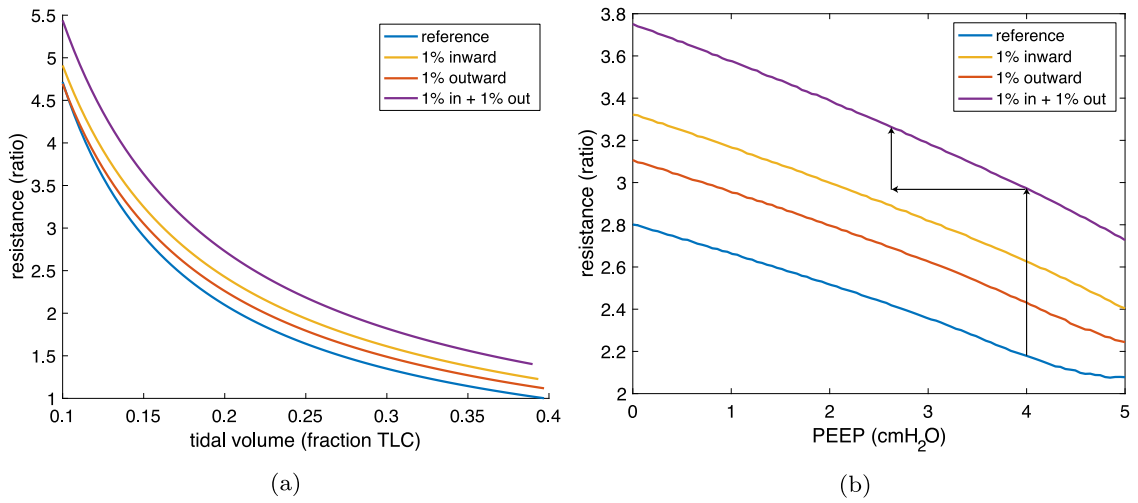

Fig. 3. Predictions of total airway resistance as tidal volume and PEEP are varied. Panel (a): PEEP of 5 cm H_2O as tidal volume is varied; (b): tidal volume of 0.2 TLC as PEEP is varied. The annotations in (b) illustrate the potential for adipose tissue in the airway wall and decreased expiratory reserve volume (decreased PEEP) to combine for a greater effect than either in isolation (see text).

tissue both in and out) has a bistable width (i.e. over which region II exists) of $\approx$ 1.6 cm H_2O. For 1% in + 1% out, (purple in panels (a)–(c)), there is a 25% increase in width of the bistable region, and for 2% in each direction, a 48% increase. The width of the region of bistability increases with both inward and outward adipose tissue, with a somewhat stronger effect in the inward direction.

A natural question is how such a change in the bistable properties of the terminal airways would manifest at lung scale. One approach is to follow Anafi and Wilson (2001) and simply partition the lung between terminal airways in the two possible stable solutions according to the target tidal volume for the lung as a whole; then the corresponding airway luminal radii can be used to calculate an estimate of the resistance of the lung. That is, for fixed P_{aw}^{max} and a target lung tidal volume $\hat{v}$, use Fig. 2(c) to find the two stable terminal tidal volumes (say v_1 and v_2), and then partition the terminal units of the lung as necessary to meet the overall volume: $\alpha = (\hat{v} - v_2)/(v_1 - v_2)$, where α is the fraction of the terminal units in v_1 (and thus $(1-\alpha)$ is the fraction in v_2).

The resulting resistance calculations, as tidal volume and PEEP are varied, are shown in Fig. 3, for the reference configuration as well as several adipose tissue configurations. This clearly illustrates the increase in resistance due to adipose tissue, but also the potential for additional contributions from volume reduction to magnify the increased resistance. There is a strong association between BMI and reduced expiratory reserve volume (Jones and Nzekwu, 2006), which in this model is most closely associated with a decrease in PEEP (shifting the tidal range lower). The annotations in the right panel (black arrows) illustrate the potential for adipose tissue in the airway wall and decreased expiratory reserve volume (decreased PEEP) to combine for a greater effect than either in isolation. That is, both adipose tissue (moving upwards) and volume changes (moving left, and then further upwards) combine synergistically into a greater effect.

One additional way to interpret this information is as the of level of external PEEP required to overcome various adipose tissue scenarios. For the tidal volume of 0.2 TLC as shown in Fig. 3(b), the required PEEP to overcome adipose tissue is approximately 2 cm H_2O for 1% inward remodelling, 3 cm H_2O for 1% outward remodelling, and 4.5 cm H_2O for 1% inward and 1% outward together. The offsets are similar for other tidal volumes (data not shown).

4. Solution procedures

In this section we discuss several possible solutions procedures for the model described above, along with their relative advantages and drawbacks. We begin with the original solution procedure as described by Anafi and Wilson (2001), which is relatively computationally intensive (given the simplicity of the model), before describing several alternatives.

In the original (Anafi and Wilson, 2001), solutions are described in terms of the intersections of the curves defined by the left- and right-hand sides of Eq. (15), where the right-hand side is defined by Eq. (9) and further back substitution of Eqs. (6), (10) and (13) and so on. This is further illustrated in Fig. 4 where we begin by plotting both sides of Eq. (15) as function of ρ_m, for different values P_{aw}^{max} and f_{adi} as labelled. The single black curve is the left-hand side, which does not depend on P_{aw}^{max} or f_{adi}. Thus we can see that the solutions occur at the intersections, and how the behaviour is altered by altering the pressure and adipose tissue thickness. Note that while each of the three upper curves (P_{aw}^{max} = 15.4 cm H_2O reference; same with 2% adipose tissue; P_{aw}^{max} = 14.2 cm H_2O reference) there are three intersections, while for the lower (P_{aw}^{max} = 14.2 cm H_2O with 2% adipose tissue) there is only one solution (occurring off-figure to the left) near airway closure.[4] Thus the addition of adipose tissue of this magnitude clearly has the potential to alter functional behaviour in an important way (as we have seen in the previous section).

Observe that this procedure first requires finding the maximum of time dependent quantities numerically, before finding the curves for a suitable range of ρ_m and locating their intersections. While such a procedure is workable at small scales, it is somewhat cumbersome and not particularly well-suited to adaptation to lung scale (e.g. Venegas et al., 2005). In this section we discuss alternative solution procedures.

There are two potential areas of improvement: first, finding the maximum of Eq. (9) without numerically evaluating the entire breathing cycle, and second, finding solutions to Eq. (15) more directly rather than finding intersections by tabulation.

We begin with the first problem: finding the time at which P_{tm} is maximum. One might, in principle, differentiate with respect to time and find critical points, but the nature of the expressions (in particular Eq. (11)) means that closed form solutions are not possible. Numerical optimisation is of course an option, but here we show that approximate solutions may be useful.

First observe that Eq. (16) is of the form

$$t^* = \underset{t}{\text{argmax}} \left[a \sin(\omega t) + f(t) \sin(\omega t - \alpha) \right] \tag{17}$$

[4] Note that Fig. 4 shows ρ_m rather than ρ_i and thus closure is not at zero. See also Figs. 2(a) and 2(b).

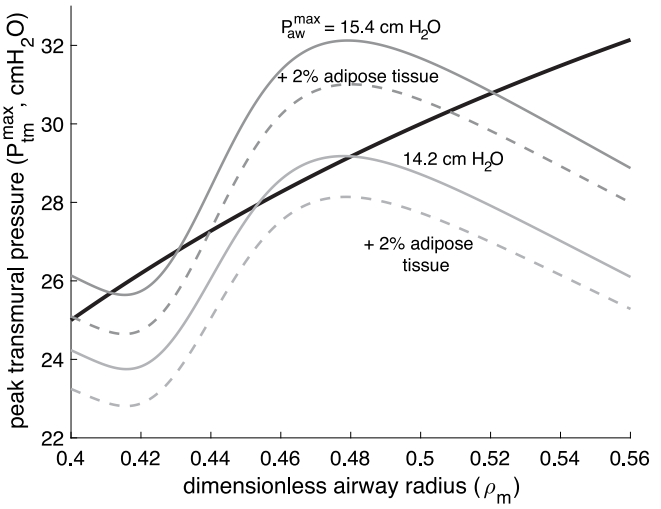

Fig. 4. Plot of both sides of Eq. (15) as function of ρ_m for different values P_{aw}^{max} and f_{adi}, labelled as the percentage of (outward) remodelling. The single black curve is the left-hand side giving the smooth muscle tension, which does not depend on P_{aw}^{max} or f_{adi}. The grey curves give the right-hand side (airway dynamics) under various conditions as labelled; model solutions occur at the intersections.

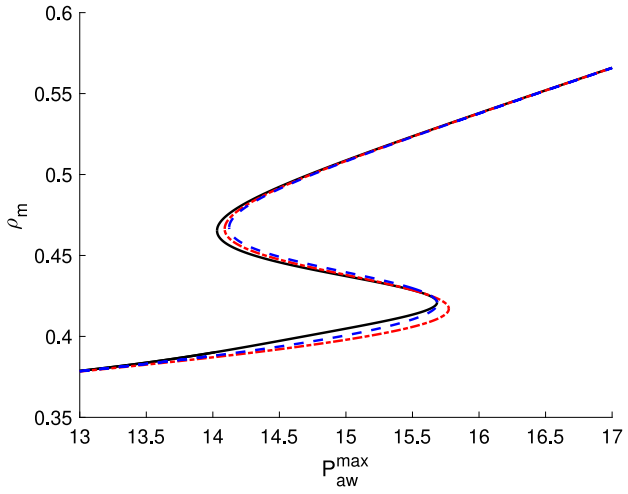

Fig. 5. Comparison of model solutions without approximation (black); using t_1^* (Eq. (21)) (blue, dashed); and t_2^* (Eq. (22)) (red, dot-dash). Typical values suggest $\bar{f} \approx 1.7$ for this parameter set. As in Fig. 2a the vertical axis is dimensionless and the horizontal in cm H_2O.

where several terms have for now been absorbed into a and $f(t)$ for clarity. The critical points then satisfy

$$\tan(\omega t - \alpha) = \frac{\omega[a\cos(\alpha) + f]}{a\omega\sin(\alpha) - \dot{f}}. \tag{18}$$

We are then interested in approximate solutions to this equation.

Here $f(t) = \frac{1}{2} + 1.4x(t) + 2.1x^2(t)$ where $x(t) = 1 - \rho_m/\sqrt[3]{v(t)}$ and $v(t)$ is sinusoidal, and so while f is not strictly sinusoidal, one is tempted to make the approximation

$$f(t) \approx c_1 + c_2\sin(\omega t - \alpha) \tag{19}$$

where the constants c_1 and c_2 can be found easily from the extrema of $f(t)$. By making such an approximation, Eq. (18) becomes (technically) solvable in closed form, but the resulting closed form expressions are so lengthy and cumbersome that numerical methods are probably preferable in most situations. However, two stronger simplifications are possible and yield more useful approximations.

The first arises from the supposition that useful closed form solutions to Eq. (18) are possible only when the right-hand side is constant. Thus assuming $\dot{f}$ is small and $\bar{f}$ is the time average, Eq. (18) becomes

$$\tan(\omega t - \alpha) = \cot(\alpha) + \frac{\bar{f}}{a\sin(\alpha)} \tag{20}$$

and so

$$t_1^* \approx \frac{1}{\omega}\left[\tan^{-1}\left(\cot(\alpha) + \frac{\bar{f}}{a\sin(\alpha)}\right) + \alpha\right] \tag{21}$$

where $a = \|P_{aw}\|/2$.

A second option is a crude but potentially useful expedient: observe that t^* lies between extrema of $\sin(\omega t)$ and $\sin(\omega t - \alpha)$. Thus one might approximate

$$t_2^* \approx (\frac{\pi}{2} + \alpha)/\omega. \tag{22}$$

The efficacy of these approximations in computing full model solutions will be demonstrated after discussing the second difficulty with the solution procedure, namely finding solutions to Eq. (15). Here there is little hope of closed form solutions, even under strong approximations. However, applying numerical root finding to Eq. (15) is much more efficient than the tabulation and intersection method described in Anafi and Wilson (2001). Here we use Powell's dog leg method (Powell, 1970) but the problem is not overly challenging and it is likely that any reasonable choice of root-finding method would be acceptable.

Combining this with the approximations found above, a comparison of model solutions is shown in Fig. 5 with model solutions without approximation (black), using t_1^* (Eq. (21)) (blue, dashed) and t_2^* (Eq. (22)) (red, dot-dash). While clearly some approximation error has been made, in many situations this may be an acceptable trade-off for much reduced computational complexity. Here t_1^* (Eq. (21)) appears to be the preferred approximation based on error alone (depending on the error measure), but recall that this also relies on an estimate of $\bar{f}$ and so may or may not be preferred, depending on the context. It is of course worth bearing in mind that even small approximation errors can potentially have outsized effects where the sensitivity is high, for example near the boundaries of the region of bistability, but in this particular application these errors are likely to be dwarfed by the uncertainty in the parameters, and indeed by other modelling assumptions. Still, these improved (and approximate) solution procedures have potential utility, in particular for coupled airway models. One further potential option would be to impose (artificial) relaxation dynamics (i.e. Donovan, 2016) on the equilibrium solutions, though this is not further explored here.

5. Discussion & conclusions

The association between obesity and increased asthma severity is most often attributed to effects of reduced lung volume. Recently, however, it has been shown that adipose tissue is also present in the airway wall itself, and that the proportion is related to BMI. This raises the possibility that functional changes at the airway level may also be important, in addition to the lung volume effects.

To date, the presence of adipose tissue has been demonstrated conclusively only in relatively large (> 6 mm) airways and has not been measured in smaller airways in humans (Elliot et al., 2019). However, adipose tissue is present throughout the airway tree – that is, both large and small airways – in animal models (Wang et al., 2023a,b). In this study we have hypothesised about the degree of adipose tissue, or other obesity-associated airway remodelling, in the smallest airways in humans, and the ways in which any such tissue might alter lung function. We have done this by modifying the model of Anafi and Wilson (2001) to include both inward and outward adipose tissue, and explored the ways in which this alters the bistability at the level of the terminal airways (which is thought to give rise to ventilation defects).

We have further estimated the resulting effect on overall resistance changes.

Adipose tissue in large airways can be of the order 1%–2% of the airway cross-sectional area (or more), and if this is also true in any substantial portion of the smallest airways there could be important functional changes. The region of bistability increases in width, and shifts rightward (with respect to airway pressure) in the presence of either inward or outward adipose tissue, and this leads to an increase in resistance and would also manifest as increased ventilation heterogeneity at the whole-lung level. It is also important to note that these changes are initially (see Fig. 2) only with respect to the airway wall adipose tissue, and no explicit effects from lung volume changes; these changes are also likely to be present, and significant, and may interact with airway level changes to amplify the effects (Macklem, 1996). While Macklem first envisaged this decrease in parenchymal tethering as a result of oedema, the same net effect can be achieved by adipose tissue. This is also compatible with the finding that obese asthma involves significant lung de-recruitment (Bates et al., 2023).

We have further demonstrated the potential for volume effects to work in concert with airway wall changes to magnify the functional impact (see Fig. 3). In short, adipose tissue within the airway wall of the distal airways may be an important contributor in understanding the relationship between obesity and asthma severity. In this manuscript we consider only the functional effect of adipose tissue in the distal airways, though it remains possible that incorporating the entire airway tree (e.g. Venegas et al., 2005) in a similar way would elucidate a similar effect in the more proximal airways.

We have considered both “inward” and “outward” adipose tissue, relative to the reference point of the smooth muscle radius. Adipose tissue in human airways has only, so far, been found in the outer wall (Elliot et al., 2019), and so the latter would seem to be more relevant than the former. There are several reasons that we have included both possible effects here. The first is that, even if adipose tissue is in fact confined to the outer wall, it remains unclear if the smooth muscle radius is indeed the relevant reference, in which case the functional effect of tissue displacement may be inward impingement upon the lumen. Second, the airway wall alterations in obesity may not be confined to adipose tissue alone, but to other types of obesity-associated airway remodelling (Scott et al., 2011). Thus accommodating both inward and outward remodelling in the model allows for both situations. Future measurements of adipose tissue within the more distal airways will then enable us to readily estimate the resulting functional effects.

As with the original (Anafi and Wilson, 2001) model, we assume PEEP as the condition of our model. This becomes most relevant when estimating the interaction with lung volume effects. The strongest volume effect in obesity is a decrease in expiratory reserve volume (ERV), without a change in tidal volume itself, thus shifting the tidal range lower (Jones and Nzekwu, 2006). In a PEEP context, the closest analogue is decreasing PEEP, which also shifts the tidal range lower. Thus in Fig. 3 we have used PEEP as a proxy for obesity-related volume changes.

Whole-lung effects have been estimated using the simple partitioning procedure of Anafi and Wilson (2001) which incorporates only the terminal units of the lung. Understanding how the patterns of the ventilation distribution change, or how adipose tissue in the more proximal airways contributes to whole-lung function, would require a model not just of the terminal units (as here) but coupling those terminal units into the airway tree (e.g. Venegas et al., 2005; Donovan, 2017). To that end we have proposed alternative solution procedures for the terminal unit model which may help to reduce the significant computational costs of the whole-lung models of bronchoconstriction.

As with any model, there are assumptions and limitations which bear further discussion. For example, although we describe the degree of additional PEEP required to overcome certain remodelling scenarios, it is important to remember that this is a model of the terminal airway unit, and not of PEEP applied to the airway tree as a whole. Similarly, wherever resistance is calculated, one must recall that we have not included proximal airways (Lutchen and Gillis, 1997; Thorpe and Bates, 1997), or chest wall mechanics (Bates, 2009), nor other obesity-induced changes in tissue resistance or reactive mechanics (Bates, 2016). For instance, the assumption of constant elastance (Eq. (5)) may also change in severe obesity (Lorx et al., 2017), but proper consideration of such a phenomenon would require a coupled-airway model. We have also considered changes in terms of airways resistance only, but it is well known that important changes occur in the (out-of-phase) reactance as well Peters et al. (2018). Finally, the use of the law of Laplace assumes a thin-walled cylinder, whereas the airway wall is in fact not particularly thin; however, it has previously been shown that the thin-walled assumption offers a reasonable approximation of the average hoop stress across a thick wall in this context (Brook et al., 2010; Hiorns et al., 2016).

In summary, we have considered the potential functional consequences of adipose tissue within the distal airway wall, and shown that if adipose tissue is present in the distal airways in quantities comparable to those found in the proximal airways, these will drive significant functional changes., namely increased resistance, airway narrowing and airway closure. Moreover these may interact with the volume effects of obesity to amplify the functional changes. The functional effects of adipose tissue in the more proximal airways remain to be studied in a coupled airway context.

CRediT authorship contribution statement

Graham M. Donovan: Conceptualization, Formal analysis, Funding acquisition, Investigation, Methodology, Project administration, Resources, Software, Validation, Visualization, Writing – original draft, Writing – review & editing. **Carolyn J. Wang:** Conceptualization, Data curation, Investigation, Writing – review & editing. **Peter B. Noble:** Conceptualization, Formal analysis, Funding acquisition, Investigation, Methodology, Project administration, Writing – review & editing. **Kimberley C.W. Wang:** Conceptualization, Formal analysis, Funding acquisition, Investigation, Methodology, Project administration, Writing – review & editing.

Declaration of competing interest

No conflicts of interest to declare.

Acknowledgements

GMD was supported by the Royal Society of New Zealand Marsden Fund, New Zealand, 22-UOA-048. KCWW has been supported by the Western Australian Future Health Research and Innovation Fund, Australia, which is an initiative of the Western Australian State Government, Australia.

References

Anafi, R.C., Wilson, T.A., 2001. Airway stability and heterogeneity in the constricted lung. J. Appl. Physiol. 91, 1185–1192.

Bates, J.H., 2009. Lung Mechanics: An Inverse Modeling Approach. Cambridge University Press.

Bates, J.H., 2016. Physiological mechanisms of airway hyperresponsiveness in obese asthma. Am. J. Respir. Cell Mol. Biol. 54, 618–623.

Bates, J.H., Bullimore, S.R., Politi, A.Z., Sneyd, J., Anafi, R.C., Lauzon, A.-M., 2009. Transient oscillatory force-length behavior of activated airway smooth muscle. Am. J. Physiol.-Lung Cell. Mol. Physiol. 297, L362–L372.

Bates, J.H., Kaminsky, D.A., Garrow, O.J., Martin, F.K., Peters, U., Tharp, W.G., Dixon, A.E., 2023. Lung de-recruitment in the allergic asthma of obesity: evidence from an anatomically based inverse model. J. Appl. Physiol. 134, 356–364.

Beuther, D.A., Sutherland, E.R., 2007. Overweight, obesity, and incident asthma: a meta-analysis of prospective epidemiologic studies. Am. J. Respir. Crit. Care. Med. 175, 661–666.

Brook, B., Peel, S., Hall, I., Politi, A., Sneyd, J., Bai, Y., Sanderson, M., Jensen, O., 2010. A biomechanical model of agonist-initiated contraction in the asthmatic airway. Respir. Physiol. Neurobiol. 170, 44–58.

Donovan, G.M., 2016. Airway bistability is modulated by smooth muscle dynamics and length-tension characteristics. Biophys. J. 111, 2327–2335.
Donovan, G.M., 2017. Inter-airway structural heterogeneity interacts with dynamic heterogeneity to determine lung function and flow patterns in both asthmatic and control simulated lungs. J. Theoret. Biol. 435, 98–105.
Donovan, G.M., 2023. Pillars of theoretical biology: Airway stability and heterogeneity in the constricted lung. J. Theoret. Biol.
Donovan, G.M., Noble, P.B., 2021. Small airways vs large airways in asthma: time for a new perspective. J. Appl. Physiol. 131, 1839–1841.
Elliot, J.G., Donovan, G.M., Wang, K.C.W., Green, F.H., James, A.L., Noble, P.B., 2019. Fatty airways: implications for obstructive disease. Eur. Respir. J. 54.
Farah, C.S., Salome, C.M., 2012. Asthma and obesity: a known association but unknown mechanism. Respirology 17, 412–421.
Hiorns, J.E., Jensen, O.E., Brook, B.S., 2016. Static and dynamic stress heterogeneity in a multiscale model of the asthmatic airway wall. J. Appl. Physiol. 121, 233–247.
Jones, R.L., Nzekwu, M.-M.U., 2006. The effects of body mass index on lung volumes. Chest 130, 827–833.
Lai-Fook, S.J., 1979. A continuum mechanics analysis of pulmonary vascular interdependence in isolated dog lobes. J. Appl. Physiol. 46, 419–429.
Lorx, A., Czövek, D., Gingl, Z., Makan, G., Radics, B., Bartusek, D., Szigeti, S., Gál, J., Losonczy, G., Sly, P.D., et al., 2017. Airway dynamics in copd patients by within-breath impedance tracking: effects of continuous positive airway pressure. Eur. Respir. J. 49.
Lutchen, K.R., Gillis, H., 1997. Relationship between heterogeneous changes in airway morphometry and lung resistance and elastance. J. Appl. Physiol. 83, 1192–1201.
Macklem, P.T., 1996. A theoretical analysis of the effect of airway smooth muscle load on airway narrowing. Am. J. Respir. Crit. Care. Med. 153, 83–89.
Mijailovich, S.M., Butler, J.P., Fredberg, J.J., 2000. Perturbed equilibria of myosin binding in airway smooth muscle: bond-length distributions, mechanics, and atp metabolism. Biophys. J. 79, 2667–2681.
Peters, U., Dechman, G., Hernandez, P., Bhatawadekar, S., Ellsmere, J., Maksym, G., 2018. Improvement in upright and supine lung mechanics with bariatric surgery affects bronchodilator responsiveness and sleep quality. J. Appl. Physiol. 125, 1305–1314.
Powell, M.J., 1970. A hybrid method for nonlinear equations. Numer. Methods Nonlinear Algebr. Equ. 87–161.
Scott, H., Gibson, P., Garg, M., Wood, L., 2011. Airway inflammation is augmented by obesity and fatty acids in asthma. Eur. Respir. J. 38, 594–602.
Skloot, G., Schechter, C., Desai, A., Togias, A., 2011. Impaired response to deep inspiration in obesity. J. Appl. Physiol. 111, 726–734.
Tgavalekos, N.T., Tawhai, M., Harris, R.S., Mush, G., Vidal-Melo, M., Venegas, J.G., Lutchen, K.R., 2005. Identifying airways responsible for heterogeneous ventilation and mechanical dysfunction in asthma: an image functional modeling approach. J. Appl. Physiol. 99, 2388–2397.
Thorpe, C.W., Bates, J.H., 1997. Effect of stochastic heterogeneity on lung impedance during acute bronchoconstriction: a model analysis. J. Appl. Physiol. 82, 1616–1625.
Venegas, J.G., Winkler, T., Musch, G., Vidal Melo, M.F., Layfield, D., Tgavalekos, N., Fischman, A.J., Callahan, R.J., Bellani, G., Scott Harris, R., 2005. Self-organized patchiness in asthma as a prelude to catastrophic shifts. Nature 434, 777–782.
Wang, K.C.W., Donovan, G.M., James, A.L., Noble, P.B., 2020. Asthma: Pharmacological degradation of the airway smooth muscle layer. Int. J. Biochem. Cell Biol. 126, 105818.
Wang, C.J., Noble, P.B., Elliot, J.G., Choi, Y.S., James, A.L., Wang, K.C.W., 2023a. Distribution, composition, and activity of airway-associated adipose tissue in the porcine lung. Am. J. Physiol.-Lung Cell. Mol. Physiol. 324, L179–L189.
Wang, C.J., Smith, J.T., Lu, D., Noble, P.B., Wang, K.C.W., 2023b. Airway-associated adipose tissue accumulation is increased in a kisspeptin receptor knockout mouse model. Clin. Sci..